Oncogene (2016), 1–15

www.nature.com/onc

ORIGINAL ARTICLE

Myoferlin regulates cellular lipid metabolism and promotes metastases in triple-negative breast cancer

A Blomme[1], B Costanza[1,2], P de Tullio[3], M Thiry[4], G Van Simaeys[5,6], S Boutry[5,7], G Doumont[5], E Di Valentin[8], T Hirano[9], T Yokobori[2], S Gofflot[10], O Peulen[1], A Bellahcène[1], F Sherer[5], C Le Goff[11], E Cavalier[11], A Mouithys-Mickalad[12], F Jouret[13], PG Cusumano[14], E Lifrange[14], RN Muller[5,7], S Goldman[5,6], P Delvenne[15], E De Pauw[16], M Nishiyama[2], V Castronovo[1] and A Turtoi[1,2,16]

Myoferlin is a multiple C2-domain-containing protein that regulates membrane repair, tyrosine kinase receptor function and endocytosis in myoblasts and endothelial cells. Recently it has been reported as overexpressed in several cancers and shown to contribute to proliferation, migration and invasion of cancer cells. We have previously demonstrated that myoferlin regulates epidermal growth factor receptor activity in breast cancer. In the current study, we report a consistent overexpression of myoferlin in triple-negative breast cancer cells (TNBC) over cells originating from other breast cancer subtypes. Using a combination of proteomics, metabolomics and electron microscopy, we demonstrate that myoferlin depletion results in marked alteration of endosomal system and metabolism. Mechanistically, myoferlin depletion caused impaired vesicle traffic that led to a misbalance of saturated/unsaturated fatty acids. This provoked mitochondrial dysfunction in TNBC cells. As a consequence of the major metabolic stress, TNBC cells rapidly triggered AMP activated protein kinase-mediated metabolic reprogramming to glycolysis. This reduced their ability to balance between oxidative phosphorylation and glycolysis, rendering TNBC cells metabolically inflexible, and more sensitive to metabolic drug targeting *in vitro*. In line with this, our *in vivo* findings demonstrated a significantly reduced capacity of myoferlin-deficient TNBC cells to metastasise to lungs. The significance of this observation was further supported by clinical data, showing that TNBC patients whose tumors overexpress myoferlin have worst distant metastasis-free and overall survivals. This novel insight into myoferlin function establishes an important link between vesicle traffic, cancer metabolism and progression, offering new diagnostic and therapeutic concepts to develop treatments for TNBC patients.

Oncogene advance online publication, 24 October 2016; doi:10.1038/onc.2016.369

INTRODUCTION

The triple-negative breast cancer (TNBC or basal-like) is a subtype of breast cancer that lacks hormone receptors and human epidermal growth factor receptor 2 (HER2). Unlike other breast cancers, which can be specifically treated either with hormone agonists (luminal-A/luminal-B) or anti-HER2 antibodies (HER2-like), TNBC has no targeted treatment resulting in worst overall and progression-free survivals.[1] The fact that TNBC treatment is an unmet need has been widely recognized by many translational studies aiming to discover new molecular targets to develop novel therapies.[2,3] Parallel to this concept, targeting metabolism of cancer cells has emerged as a promising therapeutic approach with potential consequences for many if not all types of cancer.[4] Ever since the initial observation made by Warburg,[5] the Achilles' heel of cancer cell metabolism is seen in its addiction to glycolysis and its 'injured' ability to perform respiration.[5] However, recent data show that mitochondrial oxidative phosphorylation (OXPHOS) is intact in many cancers and is probably suppressed by glycolysis rather than being defective.[6,7] We appreciate, today, the fact that tumors are heterogeneous entities comprising cancer cells with different metabolic statuses that can collaborate to optimize the exploitation of limited energy resources.[8–10] Thus, it would be very disadvantageous for the fittest cancer cells to limit their metabolism only to glycolysis. Recent data demonstrate that cancer cells can switch from glycolysis to OXPHOS as a resistance mechanism to targeted treatment.[11] Metabolic flexibility is, therefore, of an enormous importance for the cancer cell, bringing a selective advantage for survival in hostile conditions.

The two key steps at the very beginning of a physiological metabolism are nutrient uptake and growth factor signaling.[12–14] Both processes are regulated by endocytosis, a complex sequence of events that intakes the cargo in membrane vesicles and addresses these to specific locations inside the cell.[15,16] In particular, the fatty acid trafficking is essential in generating energy, whereas the excess of free fatty acids (FFA) is harmful to mitochondrial membrane integrity.[17,18] Despite the fact that our understandings of physiological conditions are expanding, the contribution of endocytosis to cancer cell metabolism and its role

[1]Metastasis Research Laboratory, GIGA Cancer, University of Liège, Liège, Belgium; [2]Department of Molecular Pharmacology and Oncology, Gunma University Graduate School of Medicine, Gunma, Japan; [3]Center for Interdisciplinary Research on Medicine, CIRM, University of Liège, Liège, Belgium; [4]Faculty of Sciences, Laboratory of Cell Biology, University of Liège, Liège, Belgium; [5]Center for Microscopy and Molecular Imaging, Charleroi, Belgium; [6]Department of Nuclear Medicine, Hôpital Erasme, Université Libre de Bruxelles, Brussels, Belgium; [7]Department of General, Organic and Biomedical Chemistry, NMR and Molecular Imaging Laboratory, University of Mons, Mons, Belgium; [8]GIGA-Viral Vectors Platform, University of Liège, Liège, Belgium; [9]Department of Molecular Pharmacology and Oncology, Gunma University Graduate School of Medicine, Gunma, Japan; [10]BIOTHEQUE, University of Liege, Liege, Belgium; [11]Department of Clinical Chemistry, University Hospital, University of Liège, Liège, Belgium; [12]Center for Oxygen Research and Development, University of Liège, Liège, Belgium; [13]GIGA Cardiovascular Sciences, University of Liège, Liège, Belgium; [14]Department of Senology, University Hospital, University of Liège, Liège, Belgium; [15]Department of Pathology, University Hospital, University of Liège, Liège, Belgium and [16]Mass Spectrometry Laboratory, University of Liège, Liège, Belgium. Correspondence: Dr A Turtoi, Metastasis Research Laboratory, GIGA Cancer, University of Liège, Avenue de l'Hopital 3, Tour Patho. +4, Liege 4000, Belgium.
E-mail: a.turtoi@ulg.ac.be
Received 27 May 2016; revised 30 July 2016; accepted 28 August 2016

in tumor progression remains unclear. This is partly because only a handful of proteins, none of them specific to cancer cells, have been identified as critical players in the process of endocytosis, and particularly vesicle traffic. In the current work, we highlight a poorly characterized protein myoferlin, which has been found prominently overexpressed in many malignancies (breast cancer,[19–21] B-cell lymphoma,[22] pancreas cancer[23–25] and lung cancer[26]) while being absent from most normal tissues.[20] Myoferlin is a 230 kDa, multiple C2-domain, ferlin family member protein, mainly known for its function in myoblast fusion as well as endocytosis in myoblast[27] and endothelial cells.[28] Our group and others have shown that myoferlin is associated with lipid raft microdomains,[28,29] and is involved in maintaining caveolae structure.[20] In cancer, myoferlin has a tumor-promoting function by increasing cancer cell proliferation, migration and invasion. However, the mechanism of action remains poorly understood and its involvement in other cancer-related processes insufficiently elucidated. We have recently demonstrated that myoferlin regulates epidermal growth factor signaling in breast cancer by affecting intracellular handling of the activated epidermal growth factor receptor.[20] Motivated by these results we have sought to investigate myoferlin expression across 51 breast cancer cell lines of different molecular subtype. The data show that myoferlin is overexpressed in the majority of TNBC cells, both at mRNA and protein level. Intrigued by these findings we assessed proteomics, metabolomics and ultrastructural changes following myoferlin suppression. We found that myoferlin is an essential component of the cellular endosomal machinery, regulating fatty acid household, mitochondrial function and, hence, global metabolism in TNBC cells. High levels of myoferlin conferred metabolic flexibility to TNBC cells, allowing them to adapt to hostile environments and, hence, increase their metastatic potential.

RESULTS

Myoferlin is highly expressed in TNBC cells and is important for the growth of TNBC xenografts *in vivo*

Owing to our previous work showing that myoferlin is overexpressed in breast cancer,[20] we first sought to refine this observation and evaluate its expression in breast cancer cells of different molecular subtypes. Therefore, we have analysed publicly deposited data[30] allowing the assessment of myoferlin mRNA expression in 51 breast cancer cell lines (Figure 1a). The analysis surprisingly demonstrated that myoferlin was overexpressed in 16 out of 26 basal-like and only 7 out of 25 luminal-like breast cancer cells. On the protein level, we have confirmed that the expression of myoferlin was higher in TNBC than in the estrogen receptor-positive and HER2-positive cancer cells (Figure 1b). We have observed two major bands at the protein level, one of which was at ~230 kDa and a second at 175 kDa. An immunoprecipitation experiment using MDA-MB-231 cells followed by mass spectrometry (MS) analysis has confirmed that both bands corresponded to myoferlin (data not shown). Database search (http://www.uniprot.org/uniprot/Q9NZM1) showed that myoferlin is alternatively spliced in several isoforms, where the 230 kDa band corresponds to canonical isoform 1, whereas the 175 kDa band to isoform 5. In TNBC the 230 kDa isoform is the dominant form of the protein and we have further focussed only on this protein band. Following this observation in cancer cell lines, we next sought to examine if TNBC tumors from breast cancer patients showed elevated levels of myoferlin expression and if this expression was limited only to epithelial cells. The examination of 30 TNBC cases (Figure 1c) demonstrated that myoferlin expression was significantly higher in tumoral regions (score 5) than the normal breast ducts (score 1); the expression was confined mainly to epithelial cells, although low expression was noted also in endothelial cells (data not shown).

Considering these findings we next asked the question if myoferlin is important for the growth of TNBC. In order to examine the impact of myoferlin on tumor growth, we have xenografted MDA-MB-231 stably depleted of myoferlin and control cells in NOD-SCID mice. Weekly measurements of primary tumor volumes indicated that silencing of myoferlin significantly decreased tumor size (Figure 1d). On average, the volumes of control tumors were ~35% larger than the ones in myoferlin-silenced tumors. The decrease of tumor volume (observed with caliper measurements, Figure 1d) was independently confirmed using magnetic resonance imaging (Figure 1f). Histological evaluation (post resection) highlighted significant differences between the control- and myoferlin-depleted tumors. Indeed, control tumors displayed a large necrotic core, which was absent in the myoferlin-silenced xenografts (Figure 1e). Furthermore, the edges of the myoferlin-silenced tumors appeared less invasive toward the surrounding muscle and fat tissue. In contrast to this, wild-type tumors showed marked zones of muscle/fat tissue infiltration by cancer cells (Figure 1e). Myoferlins' pleiotropic expression in TNBC, its impact on tumor growth and the apparent morphological differences seen in myoferlin depleted tumors suggested that myoferlin is involved in more fundamental mechanisms, beyond the ones that were previously described in breast cancer.[20,21]

OMICS analysis of myoferlin-depleted tumors *in vivo* highlights major changes in vesicle trafficking and metabolism

In order to further characterize the *in vivo* effects following myoferlin depletion, we first conducted a proteomic analysis of xenografted tumors. The MS-based analysis has identified 1682 proteins, among which 202 proteins were upregulated in the control condition, whereas 177 proteins were overexpressed in the myoferlin-deficient tumors (detailed in Supplementary Data section, Supplementary Table 1). The top five Gene Ontology biological functions that displayed strongest enrichment of the modulated proteins were vesicle trafficking, RNA/DNA binding, cytoskeleton remodeling, carbohydrate metabolism and protein synthesis (Figure 2a). Knowing the importance of myoferlin in endocytosis and vesicle trafficking, as well as the role of endocytosis in metabolism, we further focused on individual proteins that were modulated in these biological processes (Figure 2b). The proteomic analysis indicated that many vesicle-related proteins were significantly modulated in myoferlin-deficient tumors. Among these, noteworthy was the alteration of Rab GTPase proteins (RAB11A, RAB2A, RAB6A and RAB6B), which are essential for vesicle trafficking. The proteomic analysis also surfaced several members of the syntaxin family (STX6, STX7) that are important for exocytosis as well as proteins that are involved in lipid rafts (ERLIN1) and lysosomes (VPS29). Interestingly, extended synaptotagmin-2 (ESYT2), a multiple C2-domain protein involved in lipid transport, was undetectable in tumors lacking myoferlin. In addition to proteins important for vesicle trafficking, the proteomic analysis pointed at significant alteration of enzymes important for cell metabolism. The modulated proteins were involved mainly in glucose (PFKL, LDHAL6A, PKLR, PGAM4 and HK1) and lipid (DECR1, GLUD2 and ECI1) metabolism. These two metabolic processes appeared to be connected by the significant downregulation of pyruvate carboxylase, which is at the crossroad between glucose and lipid biosynthesis. Owing to these observations we next sought to examine whether these protein modulations would translate into changes of cellular metabolism. Therefore we have extracted general metabolites and lipid mediators from myoferlin-expressing and myoferlin-deficient xenografts and have performed metabolomic analysis (Figure 2c). The results for general metabolites pointed to a significant decrease of several intermediates of the tricarboxylic acid cycle (isocitric acid, succinic acid) and oxidative stress markers

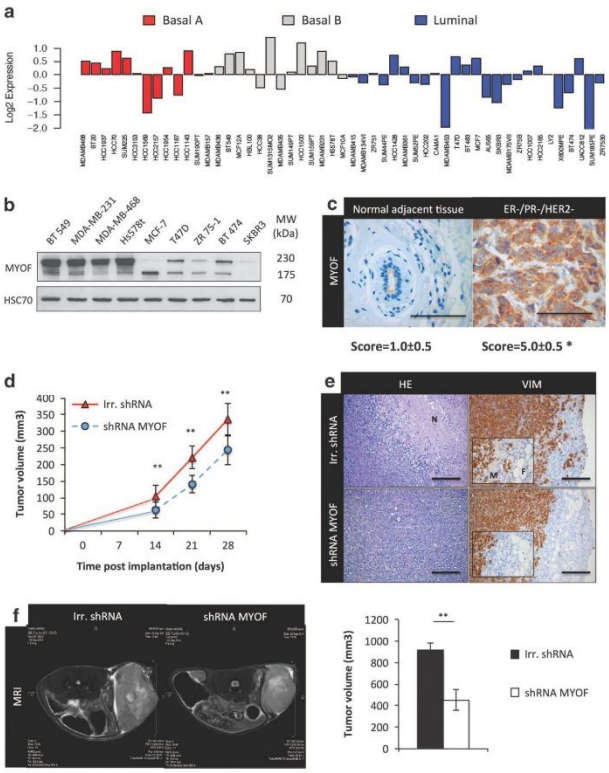

Figure 1. Myoferlin is overexpressed in TNBC cells and tumors. (**a**) Gene expression of myoferlin in 51 breast cancer cell lines; adapted from GOBO: http://co.bmc.lu.se/gobo/gsa_cellines.pl. (**b**) Western blot analysis of myoferlin expression in breast cancer cell lines. (**c**) Immunohistochemistry (IHC) analysis of myoferlin expression in normal breast tissue (adjacent non-tumoral) and ER-/PR-/HER2-tumors (TNBC). Images of representative fields were taken at ×400 magnification. The quantification of immunoreactivity is shown as a mean value with s.d. of means (s.d.), where $N = 30$ cases. Statistical significance was calculated using Mann–Whitney *U*-test where * denotes a *P*-value $\leqslant 0.05$; (**d**) Volumes (mm^3) of primary tumors following subcutaneous injection of MDA-MB-231 cells silenced for myoferlin expression (blue line) or control cells (red line). Error bars indicates s.d., where $N = 10$ tumors. Statistical significance was calculated using Student's *t*-test where ** denotes a *P*-value $\leqslant 0.01$. (**e**) Representative hematoxylin and eosin (H&E) and vimentin IHC staining in MDA-MB-231-resected xenografts. Control tumors displayed a necrotic core (N) and an evident invasion in the muscle (M) and fat (F) layers. Shown are the histological images of representative fields taken at ×100 magnification. (**f**) Representative picture of magnetic resonance imaging (MRI) of primary tumors *in vivo* (performed 4 weeks post engraftment) and quantifications of MRI volume. Error bars indicate s.d. of means ($N = 10$ tumors). Statistical significance was calculated using Student's *t*-test where ** denotes a *P*-value $\leqslant 0.01$.

(GSSG, ophthalmic acid and 4-aminobutyric acid) caused by myoferlin depletion. The level of pantothenic acid, an essential nutrient required for acetyl-CoA biosynthesis, was also decreased in the absence of myoferlin. By contrast, nucleotide-derived metabolites (NAD, cytidine, GMP and uric acid) as well as carnosine (antioxidant and anti-glycation molecule) were higher represented in myoferlin-depleted tumors. Extended metabolomic analysis focusing on lipid mediators further revealed that the large majority of these metabolites, especially derivatives from the essential polyunsaturated fatty acids such as linoleic (HODE, KODE) and arachidonic acids (HETE, KETE), were significantly downregulated or/and undetectable in tumors lacking myoferlin. Taking into account the major changes of proteins participating in endosome biology (13% of modulated proteins are participating in vesicle traffic) as well as the resulting impact on cellular metabolism, we next hypothesized that the ultrastructure of myoferlin-depleted cells would be significantly altered.

Myoferlin is expressed throughout the endosomal system and its depletion impedes vesicle trafficking in TNBC cells

In order to visualize the effects of myoferlin silencing we employed transmission electron microscopy analysis. We have first evaluated the subcellular localization of myoferlin using immunogold labeling followed by transmission electron microscopy. The labeling specificity was confirmed with MDA-MB-231 cells that were both stably and transiently transfected with short hairpin RNA (shRNA)/small-interfering RNA (siRNA) against

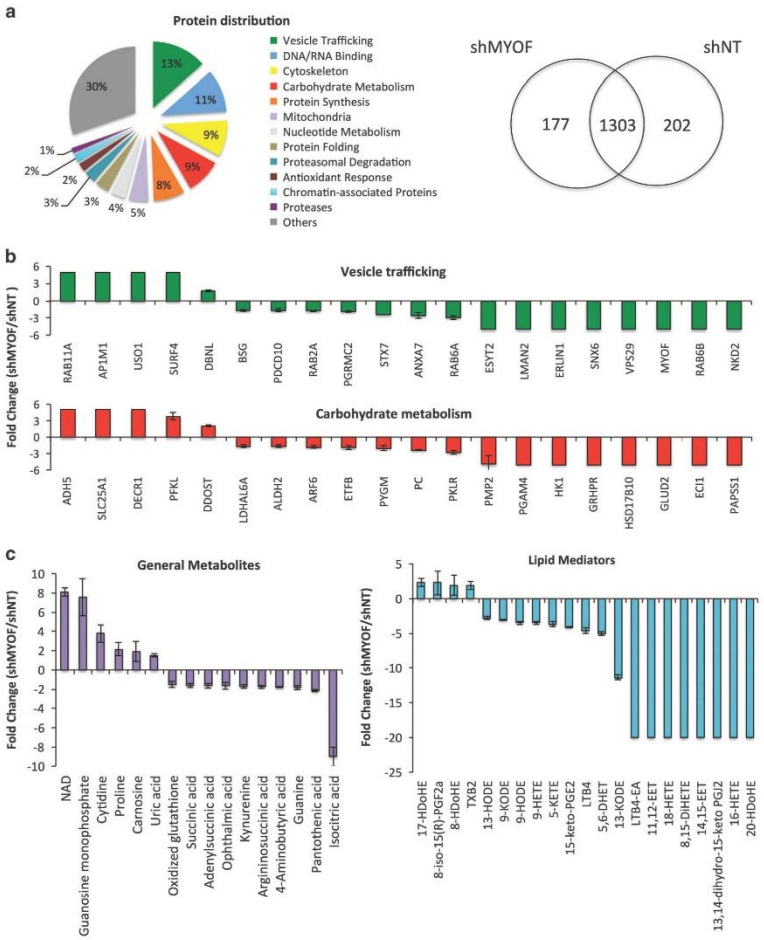

Figure 2. OMICS analysis of myoferlin-depleted MDA-MB-231 tumors evidences major impact on vesicle traffic and metabolism. (**a**) (Left panel) Distribution of modulated proteins (myoferlin-depleted (shMYOF) versus control tumors (shNT)) according to their respective association with Gene Ontology molecular function category. (Right panel) Venn diagram representing numbers of modulated proteins found in respective conditions. (**b**) Overview of top 20 modulated proteins taking part in vesicle traffic and carbohydrate metabolism. (**c**) Metabolomic analysis of general metabolites and lipid mediators; displayed are all molecules that had a fold-change ratio higher than two-fold. (**b** and **c**) Error bars indicate s.d. ($N = 5$ tumors), whereas proteins/metabolites without error bars have been uniquely identified in only one condition (they have been given a default maximum value in order to represent them in the graph).

myoferlin (data not shown). In wild-type cells, myoferlin staining was mainly localized in the cytoplasm and at the plasma membrane of the cells (Figure 3a, left panel). In the cytoplasm, myoferlin was strongly expressed in several components of the endosomal system, such as early or late endosomes, including their potential anchor sites on the plasma membrane (Figure 3a, left panel). A strong myoferlin labeling was particularly evident in trafficking vesicles such as clathrin-coated vesicles and caveolae (Figure 3a, right panel). The presence of myoferlin in caveolae reinforced previously reported co-localization data for myoferlin and caveolin-1,[20,28] and raised the possibility that myoferlin has broader roles in general vesicle trafficking. Indeed, EM results showed that MDA-MB-231 cells deficient for myoferlin were characterized by an important accumulation of vesicles near the plasma membrane (Figure 3b, black/green arrows). In the absence of myoferlin, majority of the vesicles also appeared as round and closed structures, whereas the presence of open vesicles was very frequently observed at the surface of control cells. In addition, the cells lacking myoferlin were distinguished from control cells by a reduction in size and frequency of late endosomes and lysosomes

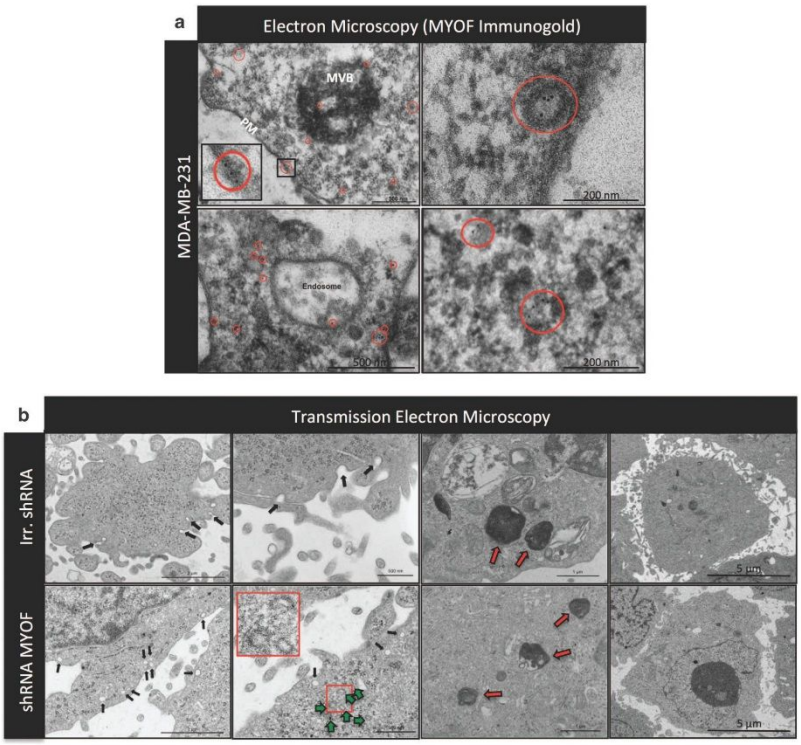

Figure 3. Myoferlin is expressed in cancer cell endosomes and its depletion affects vesicle traffic. (**a**) TEM (transmission electron microscopy) analysis of anti-myoferlin immunogold labeling in MDA-MB-231 highlighted, in addition to the membrane labeling, the specific localization of the protein within the endosomal system and in trafficking vesicles (including clathrin-coated vesicles and caveolae). Magnification highlights membrane myoferlin labeling. (**b**) TEM analysis of ultrastructural changes following stable myoferlin depletion in MDA-MB-231. Myoferlin silencing resulted in accumulation of vesicles in the vicinity of the plasma membrane. MDA-MB-231 cells lacking myoferlin displayed an important accumulation of vesicles notably caveolae (green arrows, high magnification) and closed-state clathrin-coated vesicles (black arrows) near to the cell membrane. Decrease in the number and the size of late-endosomal/lysosomal structures (red arrows) and a reduction in the number of microvilli have also been frequently observed. Representative images of at least three independent replicates are shown. PM, plasma membrane; MVB, Multi-vesicular body.

(Figure 3b, red arrows). Finally, cells without myoferlin displayed a marked decrease in the number of microvilli (Figure 3b, right panel, lower magnification). These observations are in agreement with the proteomic data, showing that myoferlin silencing induces a major disruption of vesicular trafficking between the plasma membrane and the endosomal compartment in cancer cells. Considering the OMICS data from the Figure 2 and structural data from the Figure 3, we further hypothesized that these two events are causally connected. Thus, we sought to further elucidate the possible mechanisms that connect myoferlin-induced endosomal effects and metabolic perturbations in TNBC tumors. Accordingly, we have further investigated *in vitro* the effect of myoferlin silencing on various metabolic parameters of TNBC cells.

Myoferlin-dependent impairment of vesicle trafficking results in an unbalanced cellular household of lipids and fatty acids

Considering the role of the endosomal system in cell metabolism,[31] we began our evaluation of the impact of myoferlin depletion in TNBC cells by performing nuclear magnetic resonance (NMR)-based metabolomic analysis. The analysis was performed on MDA-MB-231 cells that were stably depleted of myoferlin (shRNA) and their control counterparts. The principal component analysis of the intracellular metabolomics profiling data showed a significant discrimination between myoferlin-deficient and control cells based on the enrichment of lipid-containing compounds and glycoproteins (Figure 4a). Further quantitative NMR-based evaluation of the global lipid-enriched fraction confirmed significantly higher levels of lipids in cells deficient in myoferlin (Figure 4a). Because NMR-based metabolomics does not allow a precise identification of the modulated lipid compounds, we conducted gas chromatograpy analysis to evaluate the specific changes of FFA inside the cancer cells. The gas chromatograpy results confirmed that myoferlin-depleted cells displayed on average 35% more intracellular FFA than their control counterparts, evidencing also an increased proportion of mono unsaturated fatty acids (Figure 4b). Quantification of

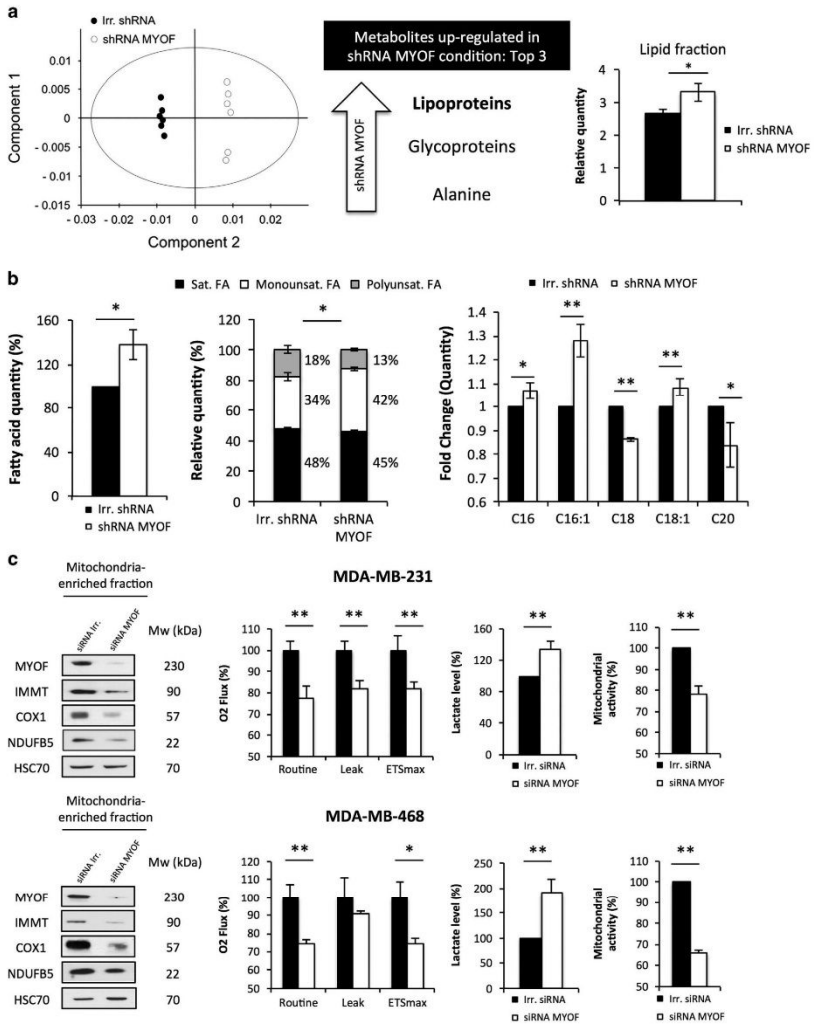

Figure 4. Myoferlin silencing alters lipid balance, affects mitochondrial function and causes metabolic reprogramming in TNBC cells. (**a**) NMR-based metabolomics of intracellular metabolites obtained by comparing stably transfected MDA-MB-231 with MYOF (white) or CTRL (black) shRNAs ($n=6$). Score plots are shown for PC1 versus PC2 from the principal component analysis (PCA) model. Top three discriminant metabolites highlighted changes in lipid metabolism between the two cell lines. NMR semi-quantitative analysis of lipid-enriched fraction (right panel) confirmed the accumulation of lipid-based molecules in myoferlin-depleted cells. (**b**) Gas chromatograpy analysis of free fatty acid (FFA) reveals that cells lacking myoferlin display higher quantity of FFA but also a higher proportion of mono unsaturated FFA. Relative quantification of representative FFA is illustrated (right panel). (**c**) Western blot analysis on mitochondria-enriched fraction of MDA-MB-231 and MDA-MB-468 cells showed that the expression level of several mitochondrial proteins is reduced upon myoferlin silencing. Images are representative of three independent experiments; HSC70 was used as a loading control. Oxygen consumption, NMR-based quantification of extracellular lactate in cell culture media and WST-1 assay suggested that a shift toward glycolysis occurred in TNBC cell lines upon myoferlin silencing. Cellular respiration was measured in culture medium (Routine), in the presence of oligomycin (Leak) or after uncoupling with FCCP (ETSmax). All values were corrected for residual oxygen consumption obtained in the presence of rotenone. Error bars indicate s.d. of means from minimum three independent biological replicates. Statistical significance (P) was evaluated using an unpaired Student t-test (*P-value $\leqslant 0.05$; **P-value $\leqslant 0.01$).

individual FFA highlighted a significant enrichment of several FFA classes in myoferlin-depleted cells (Figure 4b). The global accumulation of fatty acids was mainly due to cellular enrichment of the relatively abundant palmitic (C16) and oleic (C18:1) acids (both account for 55% of all fatty acids), in myoferlin-deficient cells when compared with controls (Figure 4b). Interestingly, increased ratio of mono unsaturated/saturated fatty acids in cells lacking myoferlin mainly resulted from conversion of stearic acid (C18) to oleic acid (C18:1). In contrast to this, the proportion of polyunsaturated fatty acids was significantly decreased in myoferlin-deficient cells. Increased cellular levels of lipids and fatty acids, including changes in their saturation, are known to be detrimental to mitochondrial structure and, hence, function.[32] This has motivated us to further examine if myoferlin deficiency could affect mitochondrial function.

Myoferlin silencing in TNBC cells causes mitochondrial dysfunction and metabolic reprogramming

In order to have a general readout concerning the impact of myoferlin loss on mitochondrial function, we have first isolated mitochondria from TNBC cells (MDA-MB-231 and MDA-MB-468). We have then tested the levels of different mitochondrial markers involved in the respiratory chain (NDUFB5, COX1) or mitochondrial structure (IMMT). As shown in Figure 4c, mitochondria of myoferlin-deficient cells displayed a significantly decreased expression of all the proteins tested. The resulting impact on mitochondrial activity was further examined by measuring oxygen consumption rate in myoferlin-deficient versus control cells. The basal respiration of the cells was measured in the culture medium (reported here as 'routine respiration') as well as in presence of oligomycin (referred here as 'leak') and FCCP (called 'electron transport system'—ETSmax). Myoferlin silencing resulted in decreased oxygen consumption rate, both basal and leak, and in reduced total capacity of the respiratory chain (Figure 4c). The consequence of the decreased mitochondrial function was balanced by increased glycolysis, resulting in higher extracellular lactate levels (Figure 4c). Myoferlin-depleted cells also showed a decreased ability to cleave WST-1 tetrazolium salt to formazan dye, suggesting that these cells displayed a lower mitochondrial dehydrogenases activity (Figure 4c). In addition, measurements of the cellular ATP and mitochondrial reactive oxygen species (ROS) levels indicated that cells lacking myoferlin also generated less ATP and exhibited a decreased production of the mitochondrial superoxide anion (Supplementary Figure S1). The mitochondrial dysfunction and metabolic shift toward glycolysis were confirmed using a second siRNA directed against myoferlin (Supplementary Figure S2). On the basis of these findings we have postulated that the shift of TNBC cells to glycolysis could be a rescue mechanism to avoid cell death. We, therefore, expected that TNBC cells lacking myoferlin would induce pathways contributing to energy preservation. To test this we have first examined whether the metabolic sensor AMPK was activated upon myoferlin depletion.

Myoferlin silencing activates the metabolic sensor AMPK and stabilizes HIF1A under normoxia

As shown in Figure 5a, myoferlin depletion in four different TNBC cell lines induced strong phosphorylation of AMPK. This activation was confirmed using a second siRNA (Supplementary Figure S2) and appeared additionally sustained by the induction of AMPK protein expression (Figure 5b). Activation of AMPK signaling promotes glycolysis as an ATP-generating pathway and inhibits ATP-consuming processes such as lipid or protein synthesis. As predicted by our initial hypothesis, myoferlin-dependent AMPK activation induced the phosphorylation of its downstream target acetyl-coA carboxylase (ACC) (Figure 5b). Phosphorylated ACC inhibits lipogenesis, contributing toward reducing the energy consumption of myoferlin-deficient cancer cells. Another AMPK target that was evidently altered following myoferlin depletion was HIF1A (Figure 5b). HIF1A regulates several cellular processes required for survival under hypoxic conditions, one of which being glycolysis. Surprisingly, myoferlin depletion induced HIF1A stabilization under normoxic conditions. Further to this, myoferlin silencing in MDA-MB-231 and MDA-MB-468 cells also caused a decrease in the expression level of the mitochondrial cytochrome *c* oxidase subunit 1 (COX1) and a marked increase in the phosphorylation of pyruvate dehydrogenase (pPDH) (Figure 5b). Consistent with this was the observed increase of the pyruvate dehydrogenase kinase (PDHK1), the kinase responsible for phosphorylating PDH. Increase in the pPDH/PDH ratio reflected a progressive inactivation of the PDH, suggesting a general decrease in mitochondrial function. Following these observations we next aimed to assess if the observed metabolic reprogramming gave an advantage or disadvantage to cancer cells to resist treatments that target metabolism. In doing so, we wished to understand the dispensability of myoferlin contribution to cellular metabolism of TNBC.

Myoferlin silencing sensitizes cells to drugs targeting metabolism

Knowing that mitochondrial dysfunction generally leads to increased apoptosis, we first sought to evaluate whether myoferlin loss was associated with apoptosis and cell death. Using annexin-V/PI staining we observed that myoferlin-depleted MDA-MB-231 and MDA-MB-468 cells, 48 h post transfection, displayed a modest increase in early and late apoptosis compared with control cells (Figure 5c, left panel). This increase in cell death was also confirmed using the measurement of the mitochondrial membrane potential (Figure 5c, right panel). On the basis of the existing data and the hypothesis that cancer cells lacking myoferlin adapted their metabolism by activating AMPK and switching to glycolysis, we aimed to test if (a) forcing cells to continue through the tricarboxylic acid cycle and OXPHOS or (b) blocking AMPK activation may enhance cell death. Redirecting cell metabolism toward OXPHOS with dichloroacetic acid (DCA), an inhibitor of PDH kinase, significantly enhanced the effect of myoferlin silencing on both apoptosis and mitochondrial depolarization (Figure 5c). Similarly, the inhibition of AMPK activation using dorsomorphin (compound C) in myoferlin-deficient cells led to an important pro-apoptotic effect and to a significant increase in mitochondrial depolarization in comparison with control cells (Figure 5d). Taken together, these results underscored myoferlin importance in TNBC cell metabolism and demonstrated that its loss is detrimental to cancer cells. Considering that AMPK activation and HIF1A stabilization were hallmarks of this myoferlin-induced metabolic inefficiency in TNBC cells, we were motivated to verify if this was also the case in patient material.

Low myoferlin expression correlates with AMPK activation and HIF1A stabilization in tumors from TNBC patients

To examine whether myoferlin deficiency results in AMPK activation and HIF1A stabilization in TNBC tumors, we performed immunofluorescence analysis on patient material from 10 cases. The tissues were probed with anti-MYOF, anti-pAMPK and anti-HIF1A antibodies (Figure 6). Following the image acquisition, we have segmented the image into regions with high and low myoferlin expression and have quantified pAMPK and HIF1A levels. The analysis evidenced a significant inverse relationship between myoferlin expression and pAMPK/HIF1A levels, overall confirming the effects seen *in vitro* (Figures 5a and b). On the basis of this analysis we next asked the question if myoferlin expression levels in TNBC tumors correlate with patient clinical outcome. To answer this we sought to examine tumoral progression in a murine model of TNBC as well as to retrospectively analyze TNBC patient survival in relationship to myoferlin expression.